Stability of two-step spline collocation methods for initial value problems for fractional differential equations

Angelamaria Cardone[a,*], Dajana Conte[a], Beatrice Paternoster[a]

[a] *Dipartimento di Matematica, Università di Salerno, Via Giovanni Paolo II n.132, I-84084 Fisciano (Salerno), Italy*

Abstract

This paper analyzes the numerical stability of a class of two-step spline collocation methods for initial value problems for fractional differential equations. The stability region is characterized in terms of the eigenvalues of a power series, which depends on the method parameters. We provide the stability regions of several methods. Numerical experiments prove the effectiveness of the stability results both in a constant stepsize framework and in the case of graded meshes.

Keywords: fractional differential equations, spline collocation, two-step, stability, difference equations

2010 MSC: 34A08, 65R20, 65L07, 39A30

1. Introduction

We consider the initial value problem for the fractional differential equation (FDE) of the form

$$\begin{cases} D^{\alpha} y(t) = f(t, y(t)), & 0 \le t \le b \\ y^{(i)}(0) = \gamma_i, & i = 0, \dots, n-1 \end{cases} \tag{1.1}$$

*Corresponding author

Email addresses: ancardone@unisa.it (Angelamaria Cardone), dajconte@unisa.it (Dajana Conte), beapat@unisa.it (Beatrice Paternoster)

where $n-1 < \alpha < n$, $n \in \mathbb{N}$, $f : [0,b] \times \mathbb{R} \to \mathbb{R}$ is a continuous function, $\gamma_i \in \mathbb{R}$. Here $D^\alpha y$ is the Caputo-type fractional derivative:

$$D^\alpha y(t) = \frac{1}{\Gamma(n-\alpha)} \int_0^t \frac{y^{(n)}(s)}{(t-s)^{\alpha+1-n}} ds.$$

Several problems in science and engineering may be modeled by FDEs (see, for example, [1–3] and references therein). In last decades many efforts have been made to develop accurate and efficient numerical schemes. Here we just mention methods of Adams type, also within predictor corrector schemes [4–7], collocation methods [8–19], Adomian decomposition methods [20], variational iteration methods [21–23] implicit-explicit schemes [24].

Here we consider spline collocation methods. This class of methods is widely applied for evolutionary problems like ordinary differential equations and integral equations [25–27]. Some seminal papers in this field are given by [28–30]. Several scientists proposed suitable extension of these methods to FDEs (see, for example, [9, 11–18, 31–35]). One of the main advantages consists in the fact that spline collocation methods may have high order of convergence, differently from most numerical methods for FDEs.

To be more specific, we focus our attention on the class of spline collocation methods introduced and analyzed in [9, 15–18, 32, 34]. For these methods, although a well established convergence theory is available, a study on numerical stability was still missing, at the best of our knowledge. With the aim of filling this gap, in [33], we analyzed stability of one-step spline collocation (OSSC) methods introduced in [17] and now we deal with two-step spline collocation (TSSC) methods introduced in [9]. The application of both type of methods to the linear basic test equation gives rise to recurrence relations of unbounded order. The study of the asymptotic behavior of the solution of such difference equations can be carried out by formal power series [36–38]. In [33], by suitable mathematical manipulations, the stability region of OSSC methods [17] was completely characterized on the basis of stability results for analogous methods for Abel-Volterra integral equations, studied in [36, 37]. In the case of TSSC methods, we need to restate all the results necessary to develop stability theory.

Within this theoretical framework, we construct the stability regions of several methods and verify stability results on some significant test problems.

The paper is structured as follows. In Sec. 2 some existence and uniqueness results are stated, and an integral reformulation of problem (1.1) is obtained. In Sec.3 we briefly illustrate TSSC methods, recall their convergence properties and develop the corresponding stability theory. In Sec. 4 we construct a number of stability regions. Some numerical experiments are illustrated in Sec. 5. We draw some conclusions in the last section.

2. Preliminary material

Specialized literature offers several existence and uniqueness results for linear and nonlinear FDEs, compare, e.g., monographs: [1, 3, 39]. For the analysis of spline collocation methods, it is useful to recall an existence and uniqueness result in the Banach space $C^{q,\nu}$. This and further material may be found in [15–18, 26].

Definition 2.1. $C^{q,\nu}(0,b]$, with $q \in \mathbb{N}$ and $\nu \in (-\infty, 1)$, is the space of the functions $y \in C[0,b]$, which are q times continuously differentiable in $(0,b]$, and:

$$|y^{(i)}(t)| \leq c \begin{cases} 1, & \text{if } i < 1-\nu \\ 1+|\log t|, & \text{if } i = 1-\nu \\ t^{1-\nu-i}, & \text{if } i > 1-\nu \end{cases}, \qquad t \in (0,b], \quad i = 1, \ldots, q.$$

The following theorem provides sufficient conditions which guarantee that the solution y of the problem (1.1) and its fractional derivative $D^\alpha y$ belong to the space $C^{q,\nu}(0,b]$.

Theorem 2.1. *[Th.2.1 of 17] Let $\alpha > 0$. Let $f : [0,b] \times \mathbb{R} \to \mathbb{R}$ be a continuous function, q times ($q \in \mathbb{N}$) continuously differentiable in $\Omega := (0,b] \times \mathbb{R}$, whereby there exists $\nu \in [1-\alpha, 1)$, such that for all nonnegative integers i and j, with*

$i + j \le q$, and for all $(t, y) \in \Omega$ the following estimation holds:

$$\left| \frac{\partial^{i+j}}{\partial t^i \partial y^j} f(t,y) \right| \le \psi(|y|) \begin{cases} 1, & \text{if } i < 1-\nu, \\ 1 + |\log t|, & \text{if } i = 1-\nu, \\ t^{1-\nu-i}, & \text{if } i > 1-\nu. \end{cases}$$

For $\alpha \in (0,1)$, we assume additionally that

$$\left| \frac{\partial^{i+j}}{\partial t^i \partial y^j} [f(t,y_1) - f(t,y_2)] \right| \le \psi(\max\{|y_1|,|y_1|\}) |y_1 - y_2| \begin{cases} 1, & \text{if } i = 0, \\ t^{1-\nu-i}, & \text{if } i > 0, \end{cases}$$

for all (t, y_1) and (t, y_2) belonging to Ω. The function $\psi : [0, \infty) \to \mathbb{R}$ is assumed to be monotonically increasing. Finally, suppose that the initial value problem (1.1) possesses a solution $y \in C[0, b]$ such that $D^\alpha y \in C[0, b]$.
Then $y \in C^{q,\nu}(0, b]$ and $D^\alpha y \in C^{q,\nu}(0, b]$.

Now, we introduce an integral reformulation of the problem (1.1). By setting $z = D^\alpha y$, the solution of (1.1) may be expressed as

$$y = J^\alpha z + Q, \tag{2.1}$$

where

$$(J^\alpha z)(t) = \frac{1}{\Gamma(\alpha)} \int_0^t (t-s)^{\alpha-1} z(s)\, ds, \quad t > 0, \tag{2.2}$$

$$Q(t) = \sum_{i=0}^{\lceil \alpha \rceil - 1} \frac{\gamma_i}{i!} t^i, \tag{2.3}$$

$\lceil \alpha \rceil$ being the least integer not less than α. Function z satisfies the following equation:

$$z = f(t, J^\alpha z + Q). \tag{2.4}$$

3. Numerical stability analysis of a two-step spline collocation method

In this section, first we illustrate the construction and report main convergence properties of TSSC methods proposed in [9]. Then, we analyze the numerical stability.

Let us consider the space of piecewise polynomial functions $S_k^{(-1)}(I_N)$:

$$S_k^{(-1)}(I_N) = \left\{ v : v|_{\sigma_j} \in \pi_k,\ j = 1, \ldots, N \right\}, \tag{3.1}$$

where π_k is the space of algebraic polynomials of degree not exceeding k and $I_N = \{0 = t_0 < \cdots < t_N = b\}$ is a mesh on $[0, b]$, with

$$h_j = t_j - t_{j-1}, \quad \sigma_j = [t_{j-1}, t_j], \quad j = 1, \ldots, N.$$

We introduce the collocation points

$$t_{jk} = t_{j-1} + \eta_k h_j, \quad k = 1, \ldots, m,\ j = 1, \ldots, N, \tag{3.2}$$

where

$$0 \leq \eta_1 < \eta_2 < \cdots < \eta_m \leq 1, \tag{3.3}$$

are fixed collocation parameters such that $(\eta_1, \eta_m) \neq (0, 1)$. The approximated solution of (2.4), computed by the TSSC method is the piecewise polynomial $v \in S_{2m-1}^{(-1)}(I_N)$, given by

$$v(t) = v_1(t) + \sum_{l=2}^{N} \left(\sum_{k=1}^{m} z_{lk} L_{l,m+k}(t) + \sum_{k=1}^{m} z_{l-1,k} L_{lk}(t) \right), \quad t \in [0, b], \tag{3.4}$$

where

- $z_{jk} = v(t_{jk}),\ k = 1, \ldots, m$;
- $L_{l,\mu}(t)$ is the μ-th Lagrange fundamental polynomial with respect to the points $\{t_{l-1,k}, t_{lk} \mid k = 1, \ldots, m\}$, for $t \in [t_{l-1}, t_l]$, and $L_{l\mu}(t) = 0$, for $t \notin [t_{l-1}, t_l]$, $\mu = 1, \ldots, 2m$, $l = 2, \ldots, N$;
- function v_1 is defined by a suitable starting procedure and $v_1(t) = 0$, $t \in (t_1, b)$.

We explicitly observe that

$$z_{1k} = v_1(t_{1k}). \tag{3.5}$$

By imposing that the collocation solution $v(t)$ satisfies the FDE (1.1) at the collocation points, we get the nonlinear system

$$z_{jk} = f\left(t_{jk}, (J^\alpha v)(t_{jk}) + Q(t_{jk})\right), \quad k = 1, \ldots, m, \tag{3.6}$$

which can be more explicitly written as

$$z_{jk} = f\left(t_{jk}, (J^\alpha v_1)(t_{jk}) + \sum_{\mu=1}^{m} z_{j\mu}(J^\alpha L_{j,m+\mu})(t_{jk}) + \sum_{l=2}^{j-1}\sum_{\mu=1}^{m} z_{l\mu}(J^\alpha L_{l,m+\mu})(t_{jk}) + \sum_{\mu=1}^{m} z_{j-1,\mu}(J^\alpha L_{j\mu})(t_{jk}) + \sum_{l=2}^{j-1}\sum_{\mu=1}^{m} z_{l-1,\mu}(J^\alpha L_{l\mu})(t_{jk}) + Q(t_{jk})\right), \quad (3.7)$$

$k = 1, \ldots, m$, by taking into account that $(J^\alpha L_{l\mu})(t_{jk}) = 0$ when $l > j$. Finally, the numerical solution of equation (1.1) is:

$$y_N = J^\alpha v + Q. \quad (3.8)$$

A matrix compact formulation of the method and implementation details are available in [34].

A crucial ingredient to obtain high order of convergence is given by the use of a graded mesh, i.e.

$$t_j = T\left(\frac{j}{N}\right)^r, \qquad j = 0, \ldots, N, \quad (3.9)$$

where the real value $r \geq 1$ is called grading exponent. As a matter of fact, when r is appropriately set, TSSC achieves an error decay rate of $O(N^{-2m})$, as stated in the following theorem.

Theorem 3.1. *[9] Let the problem* (1.1) *have a solution* $y \in C[0,T]$ *such that* $D^\alpha y \in C[0,T]$*, let* $f : [0,T] \times \mathbb{R} \to \mathbb{R}$ *be a continuous function such that its derivatives* $\frac{\partial}{\partial t} f(t,y)$ *and* $\frac{\partial^2}{\partial t^2} f(t,y)$ *are continuous in* $(0,T] \times \mathbb{R}$ *and*

$$\left|\frac{\partial^j}{\partial y^j} f(t,y)\right| \leq \psi(|y|), \quad (t,x) \in (0,T] \times \mathbb{R}, j = 0,1,2,$$

where $\psi : [0,\infty) \to \mathbb{R}$ *is a monotonically increasing function. Moreover assume that the collocation points* (3.2) *with grid points* (3.9) *and arbitrary parameters* $\eta_1, \ldots, \eta_m$ *satisfying* (3.3) *are used. Then there exist* $N_0 \in \mathbb{N}$ *and* $\delta_0 > 0$ *such that, for all* $N \geq N_0$*, there exists a unique two-step collocation solution* $v \in S^{(-1)}_{2m-1}(I_N)$ *in the ball* $\|u - z\|_\infty \leq \delta_0$*, where* $z = D^\alpha y \in C[0,T]$*. If, in addition, the assumptions of Th. 2.1 with* $q := 2m$ *and* $\nu \in [1-\alpha, 1)$ *are fulfilled, then for all* $N \geq N_0$ *the following error estimate holds:*

$$\|y_N - y\|_\infty \leq c E_N(2m, \nu, r),$$

with y_N given by the formula (3.8). *Here c is a constant not depending on N, $r \in [1, \infty)$ is the grading exponent in* (3.9) *and E_N is defined as follows*

$$E_N(p, \nu, r) = \begin{cases} N^{-r(1-\nu)}, & \text{if } 1 \leq r < \frac{p}{1-\nu}, \\ N^{-p}(1 + \log N), & \text{if } r = \frac{p}{1-\nu} = 1, \\ N^{-p}, & \text{if } r = \frac{p}{1-\nu} > 1 \text{ or } r > \frac{p}{1-\nu}. \end{cases} \tag{3.10}$$

For the following analysis, we recall that c_0 is the space of sequences converging to zero; ℓ^∞ is the space of bounded sequences; ℓ^1 is the space of sequences $\{x_n\}_n$ with

$$\sum_{n=0}^{\infty} |x_n| < \infty.$$

The basic linear test equation in the study of stability of numerical methods for FDEs is the following

$$\begin{cases} D^\alpha y(t) = \lambda y(t), \quad t \geq 0 \\ y(0) = y_0 \end{cases} \tag{3.11}$$

where $\alpha > 0$. The analytical solution of (3.11) is $y(t) = E_\alpha(\lambda t^\alpha) y_0$, where E_α is the Mittag-Leffler function, defined as $E_\alpha(t) = \sum_{k=0}^{\infty} \frac{t^k}{\Gamma(\alpha k + 1)}$ [see e.g. 3, 40]. Thus, $y(t)$ tends asymptotically to 0 as t tends to infinity if and only if $\lambda \in \Sigma_\alpha$, where [cfr. 7, 41]

$$\Sigma_\alpha = \{s \in \mathbb{C} : |\arg(s)| > \frac{\alpha}{2}\pi\}. \tag{3.12}$$

We are interested to study when the numerical solution mimics the asymptotic behavior of the analytical solution. To this aim, we consider the numerical solution of (3.11) given by the TSSC (3.4)-(3.6) for a fixed stepsize h, i.e. we put $h_j = h$, for all j (compare [37] and [33]).

We define two square matrices of dimension m, i.e. $W_j = (w_j(\eta_k, \eta_\mu))$ and

$\bar{W}_j = (\bar{w}_j(\eta_k, \eta_\mu))$, $j \geq 0$, as follows:

$$\begin{aligned} w_0(\eta_k, \eta_\mu) &= \int_0^{\eta_k} (\eta_k - \tau)^{\alpha-1} \varphi_{m+\mu}(\tau) d\tau. \\ w_j(\eta_k, \eta_\mu) &= \int_0^1 (j + \eta_k - \tau)^{\alpha-1} \varphi_{m+\mu}(\tau) d\tau, \quad j \geq 1, \end{aligned} \tag{3.13}$$

$$\begin{aligned} \bar{w}_0(\eta_k, \eta_\mu) &= \int_0^{\eta_k} (\eta_k - \tau)^{\alpha-1} \varphi_{\mu}(\tau) d\tau. \\ \bar{w}_j(\eta_k, \eta_\mu) &= \int_0^1 (j + \eta_k - \tau)^{\alpha-1} \varphi_{\mu}(\tau) d\tau, \quad j \geq 1, \end{aligned} \tag{3.14}$$

$k, \mu = 1, \ldots, m$. Here $\{\varphi_\mu\}_{\mu=1}^{2m}$ are the Lagrange fundamental polynomials corresponding to the nodes $\{\eta_1 - 1, \ldots, \eta_m - 1, \eta_1, \ldots, \eta_m\}$.

105 **Theorem 3.2.** *By applying the TSSC method* (3.4)-(3.6) *to equation* (3.11)*, we obtain the following recurrence relation*

$$\mathbf{z}_j = \frac{\lambda h^\alpha}{\Gamma(\alpha)} \sum_{l=0}^{j} A_{j-l} \mathbf{z}_l + \mathbf{b}_j, \quad j \geq 0, \tag{3.15}$$

where

$$\mathbf{z}_j = \left(\frac{z_{j+2,1}}{\lambda}, \ldots, \frac{z_{j+2,m}}{\lambda} \right)^T,$$

$$A_j = \begin{cases} W_0, & j = 0 \\ W_j + \bar{W}_{j-1} & j > 0 \end{cases}, \tag{3.16}$$

$$\mathbf{b}_j = y_0 \mathbf{e} + \mathbf{g}_j + \frac{\lambda h^\alpha}{\Gamma(\alpha)} \bar{W}_j \mathbf{z}_{-1}. \tag{3.17}$$

matrices W_j and $\bar{W}_j$ have been defined in (3.13) *and* (3.14)*, respectively. Moreover*

$$\lim_{j \to \infty} \mathbf{b}_j = y_0 \mathbf{e}. \tag{3.18}$$

Proof. If we apply the TSSC (3.4)-(3.6) with fixed stepsize h to the linear test equation (3.11), we get (compare (3.7))

$$\begin{aligned} z_{jk} = \lambda \Bigg[& (J^\alpha v_1)(t_{jk}) + \sum_{\mu=1}^{m} z_{j\mu} (J^\alpha L_{j,m+\mu})(t_{jk}) + \sum_{l=2}^{j-1} \sum_{\mu=1}^{m} z_{l\mu} (J^\alpha L_{l,m+\mu})(t_{jk}) \\ & + \sum_{\mu=1}^{m} z_{j-1,\mu} (J^\alpha L_{j\mu})(t_{jk}) + \sum_{l=2}^{j-1} \sum_{\mu=1}^{m} z_{l-1,\mu} (J^\alpha L_{l\mu})(t_{jk}) + y_0, \Bigg] \end{aligned} \tag{3.19}$$

$j \geq 2$, $k = 1, \ldots, m$, with $z_{1k} = v_1(t_{1k})$ (cfr.(3.5)).

The fractional integrals in (3.19) assume the form [compare Sec. 3 of 9]

$$
\begin{aligned}
(J^\alpha L_{j,m+\mu})(t_{jk}) &= \frac{h^\alpha}{\Gamma(\alpha)} \int_0^{\eta_k} (\eta_k - \tau)^{\alpha-1} \varphi_{m+\mu}(\tau) d\tau = w_0(\eta_k, \eta_\mu), \\
(J^\alpha L_{l,m+\mu})(t_{jk}) &= \frac{h^\alpha}{\Gamma(\alpha)} \int_0^{1} (j - l + \eta_k - \tau)^{\alpha-1} \varphi_{m+\mu}(\tau) d\tau = w_j(\eta_k, \eta_\mu), \\
(J^\alpha L_{j\mu})(t_{jk}) &= \frac{h^\alpha}{\Gamma(\alpha)} \int_0^{\eta_k} (\eta_k - \tau)^{\alpha-1} \varphi_{\mu}(\tau) d\tau = \bar{w}_0(\eta_k, \eta_\mu), \\
(J^\alpha L_{l\mu})(t_{jk}) &= \frac{h^\alpha}{\Gamma(\alpha)} \int_0^{1} (j - l + \eta_k - \tau)^{\alpha-1} \varphi_{\mu}(\tau) d\tau = \bar{w}_j(\eta_k, \eta_\mu),
\end{aligned}
$$

$\mu = 1, \ldots, m$. Now we set

$$
g_{jk} = (J^\alpha v_1)(t_{jk}) = \frac{1}{\Gamma(\alpha)} \int_0^{t_1} (t_{jk} - s)^{\alpha-1} v_1(s) ds, \ k = 1, \ldots, m, j \geq 1, \quad (3.20)
$$

where last equality holds since $v_1(t) = 0$ for $t > t_1$. Then, eq. (3.19) becomes

$$
z_{jk} = \frac{\lambda h^\alpha}{\Gamma(\alpha)} \sum_{l=2}^{j} \sum_{\mu=1}^{m} z_{l\mu} w_{j-l}(\eta_k, \eta_\mu) + \frac{\lambda h^\alpha}{\Gamma(\alpha)} \sum_{l=2}^{j} \sum_{\mu=1}^{m} z_{l-1,\mu} \bar{w}_{j-l}(\eta_k, \eta_\mu) + \lambda g_{jk} + \lambda y_0, \quad (3.21)
$$

$j \geq 2$, $k = 1, \ldots, m$. By dividing by λ, we obtain

$$
\mathbf{z}_{j-2} = \frac{\lambda h^\alpha}{\Gamma(\alpha)} \sum_{l=2}^{j} W_{j-l} \mathbf{z}_{l-2} + \frac{\lambda h^\alpha}{\Gamma(\alpha)} \sum_{l=2}^{j} \bar{W}_{j-l} \mathbf{z}_{l-3} + \mathbf{g}_{j-2} + y_0 \mathbf{e}, \qquad j \geq 2,
$$

with

$$
\mathbf{g_j} = (g_{j+2,1}, \ldots, g_{j+2,m})^T. \quad (3.22)
$$

A shift of indices j and l, yields

$$
\begin{aligned}
\mathbf{z}_j =& \frac{\lambda h^\alpha}{\Gamma(\alpha)} \sum_{l=0}^{j} W_{j-l} \mathbf{z}_l + \frac{\lambda h^\alpha}{\Gamma(\alpha)} \sum_{l=0}^{j} \bar{W}_{j-l} \mathbf{z}_{l-1} + \mathbf{g}_j + y_0 \mathbf{e}, \\
=& \frac{\lambda h^\alpha}{\Gamma(\alpha)} \sum_{l=0}^{j} W_{j-l} \mathbf{z}_l + \frac{\lambda h^\alpha}{\Gamma(\alpha)} \sum_{l=0}^{j-1} \bar{W}_{j-l-1} \mathbf{z}_l + \frac{\lambda h^\alpha}{\Gamma(\alpha)} \bar{W}_j \mathbf{z}_{-1} + \mathbf{g}_j + y_0 \mathbf{e}, \\
=& \frac{\lambda h^\alpha}{\Gamma(\alpha)} \sum_{l=0}^{j} A_{j-l} \mathbf{z}_l + y_0 \mathbf{e} + \mathbf{g}_j + \frac{\lambda h^\alpha}{\Gamma(\alpha)} \bar{W}_j \mathbf{z}_{-1},
\end{aligned}
$$

$j \geq 0$, thus (3.15) follows.

From (3.22), (3.20) and by a change of the integration variable $s = \tau h$, we get

$$
(\mathbf{g}_j)_i = \frac{h^\alpha}{\Gamma(\alpha)} \int_0^1 (j + 1 + \eta_i - \tau)^{\alpha-1} v_1(\tau h) d\tau = \frac{h^\alpha}{\Gamma(\alpha)} \left[j^{\alpha-1} \int_0^1 v_1(\tau h) d\tau + f_j(\eta_i) \right],
$$

where $\{f_j(\eta_i)\}_{j\geq 0}$ in ℓ^1. Thus $\mathbf{g}_j$ is in c_0. Analogously, the sequence $\bar{W}_j$ is in c_0. Therefore (3.18) is proved. □

Definition 3.1. The *stability region* of the TSSC method (3.4)-(3.6) is

$$\mathcal{R} = \left\{ \lambda h^\alpha \in \mathbb{C} \,\middle|\, \lim_{j\to\infty} \mathbf{z}_j = 0 \ \forall \mathbf{b}_j \text{ s.t. } \lim_{j\to\infty} \mathbf{b}_j = const \cdot \mathbf{e} \right\},$$

where $\mathbf{z}_j$ satisfies (3.15).

To analyze the stability, we will use the formal power series and consider the properties of the sequences of their coefficients. In particular, we introduce the formal power series

$$\mathbf{z}(\xi) = \sum_{n=0}^{\infty} \mathbf{z}_n \xi^n, \quad A(\xi) = \sum_{n=0}^{\infty} A_n \xi^n, \quad \mathbf{b}(\xi) = \sum_{n=0}^{\infty} \mathbf{b}_n \xi^n.$$

A TSSC is stable whenever the sequence of coefficients of $\mathbf{z}(\xi)$ belongs to c_0. Theorem 3.2 yields

$$\mathbf{z}(\xi) = \frac{\lambda h^\alpha}{\Gamma(\alpha)} A(\xi)\mathbf{z}(\xi) + \mathbf{b}(\xi),$$

thus

$$\left(I - \frac{\lambda h^\alpha}{\Gamma(\alpha)} A(\xi) \right) \mathbf{z}(\xi) = \mathbf{b}(\xi). \tag{3.23}$$

We introduce matrix $C(\xi)$

$$C(\xi) = \left(\begin{array}{c|c} I_{m-1} & \mathbf{e} \\ \hline \mathbf{0}_{1,m-1} & (1-\xi)^\alpha \end{array} \right), \tag{3.24}$$

where $\mathbf{e} = (1 \dots 1)^T \in \mathbb{R}^{m-1}$. We observe that $C(\xi)$ has coefficients in ℓ^1, since $(1-\xi)^\alpha$ is in ℓ^1 [cfr. (2.2) 38]. We consider the equation

$$C(\xi) \left(I - \frac{\lambda h^\alpha}{\Gamma(\alpha)} A(\xi) \right) \mathbf{z}(\xi) = C(\xi)\mathbf{b}(\xi). \tag{3.25}$$

Theorem 3.3 (Wiener inversion theorem, cfr. [42])**.** *If $\{a_n\}_n$ is in ℓ^1 and $a(\xi) \neq 0$ for $|\xi| \leq 1$, then the coefficient sequence of $1/a(\xi)$ is again in ℓ^1.*

Lemma 3.4. *[38] Let $(a_n)_{n\in\mathbb{N}} \in \ell^1$ and $|\xi_0| \leq 1$, then the sequence of coefficients of*

$$b(\xi) = \frac{a(\xi) - a(\xi_0)}{\xi - \xi_0}$$

are in c_0.

Lemma 3.5. *Let* $a(\eta_k,\eta_\mu)(\xi)=\sum_{j=0}^{\infty}a_j(\eta_k,\eta_\mu)\xi^j$, *where* $a_j(\eta_k,\eta_\mu)$ *is the* (k,μ)-*th element of matrix* A_j, *defined in* (3.16). *Let* $\{\mathbf{b}_j\}_{j\geq 0}$ *be a sequence of vectors satisfying* (3.18). *Then*

(i) $\dfrac{1}{\Gamma(\alpha)}a(\eta_k,\eta_\mu)(\xi)=(1-\xi)^{-\alpha}\displaystyle\int_0^1(\varphi_{m+\mu}(\tau)+\varphi_\mu(\tau))d\tau+\bar{d}(\eta_k,\eta_\mu)(\xi)$, *where the coefficient sequence of* $\bar{d}(\eta_k,\eta_\mu)(\xi)$ *is in* ℓ^1;

(ii) $\dfrac{1}{\Gamma(\alpha)}\left(a(\eta_k,\eta_\mu)(\xi)-a(\eta_m,\eta_\mu)(\xi)\right)$ *has coefficient sequence in* ℓ^1;

(iii) $\dfrac{1}{\Gamma(\alpha)}(1-\xi)^{\alpha}a(\eta_k,\eta_\mu)(\xi)$ *has coefficient sequence in* ℓ^1;

(iv) $\{(\mathbf{b}_j)_i-(\mathbf{b}_j)_m\}_{j\geq 0}$ *belongs to* c_0;

(v) $(1-\xi)^{\alpha}\displaystyle\sum_{j=0}^{\infty}(\mathbf{b}_j)_m\xi^j$ *has coefficient sequence in* c_0.

Proof. (i) Thanks to Newton's generalized binomial theorem, relations (3.16), (3.13) and (3.14) yield

$$\frac{1}{\Gamma(\alpha)}a_j(\eta_k,\eta_\mu)=\frac{j^{\alpha-1}}{\Gamma(\alpha)}\int_0^1(\varphi_{m+\mu}(\tau)+\varphi_\mu(\tau))d\tau+e_j(\eta_k,\eta_\mu),\quad j\geq 2,$$

where $\{e_j(\eta_k,\eta_\mu)\}_{j\geq 2}\in\ell^1$. From [(2.2)-(2.4) 38], it results

$$\sum_{j=0}^{\infty}\frac{j^{\alpha-1}}{\Gamma(\alpha)}\xi^j=(1-\xi)^{-\alpha}+d(\xi),$$

where the coefficient sequence of $d(\xi)$ is in ℓ^1. Therefore (i) holds, since

$$\bar{d}(\eta_k,\eta_\mu)(\xi)=\left(d(\xi)-\frac{\xi}{\Gamma(\alpha)}\right)\int_0^1(\varphi_{m+\mu}(\tau)+\varphi_\mu(\tau))d\tau+e(\eta_k,\eta_\mu)(\xi),$$

with $e_j(\eta_k,\eta_\mu):=\dfrac{1}{\Gamma(\alpha)}a_j(\eta_k,\eta_\mu)$, $j=0,1$.

(ii) By exploiting (i) of this Lemma,

$$\frac{1}{\Gamma(\alpha)}\left(a(\eta_k,\eta_\mu)(\xi)-a(\eta_m,\eta_\mu)(\xi)\right)=\bar{d}(\eta_k,\eta_\mu)(\xi)-\bar{d}(\eta_m,\eta_\mu)(\xi),$$

and thesis immediately follows.

(iii) Item (i) yields

$$(1-\xi)^{\alpha}\frac{1}{\Gamma(\alpha)}a(\eta_k,\eta_\mu)(\xi)=\int_0^1(\varphi_{m+\mu}(\tau)+\varphi_\mu(\tau))d\tau+(1-\xi)^{\alpha}\bar{d}(\eta_k,\eta_\mu)(\xi).$$

The coefficient sequence of $(1-\xi)^\alpha$ belong to ℓ^1 (cfr. [38, 43]), thus (iii) is proved.

(iv) It immediately follows from (3.18).

(v) We have

$$(1-\xi)^\alpha \sum_{j=0}^{\infty} (\mathbf{b}_j)_m \xi^j =$$

$$(1-\xi)^\alpha \sum_{j=0}^{\infty} \left((\mathbf{b}_j)_m - \lim_{k\to\infty} (\mathbf{b}_k)_m \right) \xi^j + (1-\xi)^\alpha \left(\sum_{j=0}^{\infty} \xi^j \right) \lim_{k\to\infty} (\mathbf{b}_k)_m =$$

$$(1-\xi)^\alpha \sum_{j=0}^{\infty} \lim_{k\to\infty} \left((\mathbf{b}_j)_m - (\mathbf{b}_k)_m \right) \xi^j + (1-\xi)^{\alpha-1} \lim_{k\to\infty} (\mathbf{b}_k)_m.$$

The above expression has coefficient sequence in c_0. As a matter of fact, the coefficient sequence of $(1-\xi)^\alpha$ belongs to ℓ^1, $\{\lim_{k\to\infty} ((\mathbf{b}_j)_m - (\mathbf{b}_k)_m)\}_{j\geq 0}$ belongs to c_0 from (3.18), and $\ell^1 * c_0 \subseteq c_0$; finally $(1-\xi)^{\alpha-1}$ has coefficient sequence in c_0. □

Theorem 3.6. *If*

$$\det\left(C(\xi) \left(I - \frac{\lambda h^\alpha}{\Gamma(\alpha)} A(\xi) \right) \right) \neq 0, \qquad \textit{for all } |\xi| \leq 1, \tag{3.26}$$

then λh^α is in the stability region $\mathcal{R}$.

Proof. To prove that the coefficient sequence of $\mathbf{z}(\xi)$ is in c_0, we will exploit the equation (3.25). Thanks to the structure of matrix $C(\xi)$ (3.24), we get

$$\frac{1}{\Gamma(\alpha)} C(\xi) A(\xi) = \frac{1}{\Gamma(\alpha)} \begin{pmatrix} [a(\eta_k, \eta_\mu)(\xi) - a(\eta_m, \eta_\mu)(\xi)]_{\substack{k=1,\dots,m-1,\\ \mu=1,\dots,m}} \\ [(1-\xi)^\alpha a(\eta_m, \eta_\mu)(\xi)]_{\mu=1,\dots,m} \end{pmatrix}.$$

Items (ii) and (iii) of Lemma 3.5 yield that the coefficient sequence of $\frac{1}{\Gamma(\alpha)} C(\xi) A(\xi)$ is in ℓ^1. Therefore, the coefficient sequences of $\det\left(C(\xi) \left(I - \frac{\lambda h^\alpha}{\Gamma(\alpha)} A(\xi) \right) \right)$ and of $\operatorname{adj}\left(C(\xi) \left(I - \frac{\lambda h^\alpha}{\Gamma(\alpha)} A(\xi) \right) \right)$ are in ℓ^1, as they consist of combinations of sums and products of series having coefficients in ℓ^1.

From (3.26) and from the Wiener theorem 3.3,

$$\left[C(\xi)\left(I-\frac{\lambda h^\alpha}{\Gamma(\alpha)}A(\xi)\right)\right]^{-1}= \\ \frac{1}{\det\left(C(\xi)\left(I-\frac{\lambda h^\alpha}{\Gamma(\alpha)}A(\xi)\right)\right)}\operatorname{adj}\left(C(\xi)\left(I-\frac{\lambda h^\alpha}{\Gamma(\alpha)}A(\xi)\right)\right)$$

has coefficient sequence in ℓ^1.

Now let us consider the right hand side of (3.25):

$$C(\xi)\mathbf{b}(\xi)=\begin{pmatrix}\left[\sum_{j=0}^{\infty}\left((\mathbf{b}_j)_i-(\mathbf{b}_j)_m\right)\xi^j\right]_{i=1,\dots,m-1}\\ (1-\xi)^\alpha\sum_{j=0}^{\infty}(\mathbf{b}_j)_m\xi^j\end{pmatrix},$$

with $\mathbf{b}_j$ defined in (3.17). From (iv) and (v) of Lemma 3.5, it follows that $C(\xi)\mathbf{b}(\xi)$ has coefficient sequence in c_0.

Finally, from (3.25), we can conclude that the coefficient sequence of

$$\mathbf{z}(\xi)=\left[C(\xi)\left(I-\frac{\lambda h^\alpha}{\Gamma(\alpha)}A(\xi)\right)\right]^{-1}C(\xi)\mathbf{b}(\xi)$$

is in c_0, since $\ell^1 * c_0 \subseteq c_0$. Then $\lambda h^\alpha \in \mathcal{R}$. □

Let us define

$$\mathbb{L}_\mu=\int_0^1\left(\varphi_\mu(\tau)+\varphi_{m+\mu}(\tau)\right)d\tau,\quad \mu=1,\dots,m, \tag{3.27}$$

$$B:=\left(\begin{array}{c|c}I_{m-1} & -\mathbf{e}\\ \hline \mathbb{L}^T & \mathbb{L}_m\end{array}\right),\quad B^{-1}=\left(\begin{array}{c|c}I_{m-1}-\mathbf{e}\,\mathbb{L}^T & \mathbf{e}\\ \hline -\mathbb{L}^T & 1\end{array}\right), \tag{3.28}$$

where $\mathbb{L}:=(\mathbb{L}_1,\dots,\mathbb{L}_{m-1})^T$ and $\mathbf{e}=(1\dots1)^T\in\mathbb{R}^{m-1}$. The expression of B^{-1} follows by $\sum_{i=1}^{m}\mathbb{L}_i=1$.

Theorem 3.7.

$$B\frac{A(\xi)}{\Gamma(\alpha)}B^{-1}=\begin{pmatrix}D(\xi) & \mathbf{d}_1(\xi)\\ \mathbf{d}_2(\xi) & d_3(\xi)\end{pmatrix}, \tag{3.29}$$

where

$$D(\xi) = (d_{is}(\xi))_{i,s=1,\dots,m-1},\ \mathbf{d}_1 = (d_{im}(\xi))_{i=1,\dots,m-1},\ \mathbf{d}_2 = (d_{ms}(\xi))_{s=1,\dots,m-1}$$

have coefficient sequences in ℓ^1 *and* $d_3(\xi) = (d_{mm}(\xi))$*, with*

$$d_{mm}(\xi) = (1-\xi)^{-\alpha} + v(\xi), \tag{3.30}$$

where $v(\xi)$ *has coefficient sequence in* ℓ^1*. Moreover, when* $\alpha \neq 0$*,* $\vec{d_1}(1) = 0 \in \mathbb{R}^{m-1}$*.*

Proof. For $i \neq m$

$$d_{is}(\xi) = \left\{ \begin{array}{c} -\mathbb{L}_s \\ 1 \end{array} \right\} \frac{1}{\Gamma(\alpha)} \sum_{l=1}^{m} \left(a(\eta_i,\eta_l)(\xi) - a(\eta_m,\eta_l)(\xi)\right) + \left\{ \begin{array}{c} \frac{1}{\Gamma(\alpha)}\left(a(\eta_i,\eta_s)(\xi) - a(\eta_m,\eta_s)(\xi)\right) \\ 0 \end{array} \right\} \begin{array}{l} s \neq m, \\ s = m. \end{array}$$

160 The coefficient sequence of d_{is} is in ℓ^1, thanks to Lemma 3.5, item (ii).

When $i = m$ and $s \neq m$,

$$d_{ms}(\xi) = \sum_{k=1}^{m} \mathbb{L}_k \left[\frac{a(\eta_k,\eta_s)(\xi)}{\Gamma(\alpha)} - \mathbb{L}_s \sum_{l=1}^{m} \frac{a(\eta_k,\eta_l)(\xi)}{\Gamma(\alpha)} \right].$$

From item (i) of Lemma 3.5, we have

$$\begin{aligned} &\frac{a(\eta_k,\eta_s)(\xi)}{\Gamma(\alpha)} - \mathbb{L}_s \sum_{l=1}^{m} \frac{a(\eta_k,\eta_l)(\xi)}{\Gamma(\alpha)} \\ &= (1-\xi)^{-\alpha}\mathbb{L}_s + \bar{d}(\eta_k,\eta_s)(\xi) - \mathbb{L}_s \sum_{l=1}^{m} \left[(1-\xi)^{-\alpha}\mathbb{L}_l + \bar{d}(\eta_k,\eta_l)(\xi)\right] \\ &= (1-\xi)^{-\alpha}\left[\mathbb{L}_s - \mathbb{L}_s \sum_{l=1}^{m} \mathbb{L}_l\right] + \bar{d}(\eta_k,\eta_s)(\xi) - \mathbb{L}_s \sum_{l=1}^{m} \bar{d}(\eta_k,\eta_l)(\xi) \\ &= \bar{d}(\eta_k,\eta_s)(\xi) - \mathbb{L}_s \sum_{l=1}^{m} \bar{d}(\eta_k,\eta_l)(\xi), \end{aligned}$$

which is in ℓ^1, thanks to Lemma 3.5, item (i).

Finally, when $i = s = m$, by exploiting Lemma 3.5, item (i)

$$d_{mm}(\xi) = \sum_{k=1}^{m} \mathbb{L}_k \sum_{l=1}^{m} \frac{a(\eta_k, \eta_l)(\xi)}{\Gamma(\alpha)} = \sum_{k=1}^{m} \mathbb{L}_k \sum_{l=1}^{m} \left[(1-\xi)^{-\alpha} \mathbb{L}_l + \bar{d}(\eta_k, \eta_l)(\xi) \right]$$
$$= (1-\xi)^{-\alpha} + \sum_{k=1}^{m} \sum_{l=1}^{m} \mathbb{L}_k \bar{d}(\eta_k, \eta_l)(\xi).$$

Last statement can be proved as in [31] and in [36]. □

Lemma 3.8.

$$\det\left(C(\xi)(I - \lambda h^\alpha \frac{A(\xi)}{\Gamma(\alpha)} \right) \neq 0 \iff \frac{1}{\lambda h^\alpha} \text{ is not an eigenvalue of } \frac{A(\xi)}{\Gamma(\alpha)},$$

for all $|\xi| \leq 1$. *In particular, in the case* $\xi = 1$

$$\det\left(C(1)(I - \lambda h^\alpha \frac{A(1)}{\Gamma(\alpha)} \right) \neq 0 \iff \frac{1}{\lambda h^\alpha} \text{ is not an eigenvalue of } \frac{A(1)}{\Gamma(\alpha)}$$
$$\iff \frac{1}{\lambda h^\alpha} \text{ is not an eigenvalue of } D(1) \text{ and } \lambda h^\alpha \neq 0.$$

Proof. The proof is based on Theorem 3.7 and follows the lines of Lemma 3.4 by [37]. □

165 **Theorem 3.9.** *The region of stability of TSSC methods for FDEs is given by*

$$\mathcal{R} = \mathbb{C} \setminus \left\{ \lambda h^\alpha \,\middle|\, \frac{1}{\lambda h^\alpha} \text{ is an eigenvalue of } \frac{A(\xi)}{\Gamma(\alpha)} \text{ for a } \xi \in \mathbb{C} \text{ with } |\xi| \leq 1 \right\}. \tag{3.31}$$

Proof. Previous theorems already proved that

$$\mathcal{R} \supseteq \mathcal{S} := \mathbb{C} \setminus \left\{ \lambda h^\alpha \,\middle|\, \frac{1}{\lambda h^\alpha} \text{ is an eigenvalue of } \frac{A(\xi)}{\Gamma(\alpha)} \text{ for a } \xi \in \mathbb{C} \text{ with } |\xi| \leq 1 \right\}.$$

Thus it remains to prove that $\mathcal{R} \subseteq \mathcal{S}$, i.e. if $r \in \mathcal{R}$, then $\det\left(I - r \frac{A(\xi)}{\Gamma(\alpha)} \right) \neq 0$ for all $|\xi| \leq 1$. By contradiction, we assume that exists $|\xi_0| \leq 1$ such that $\det\left(I - r \frac{A(\xi_0)}{\Gamma(\alpha)} \right) = 0$. We treat separately the cases $\xi_0 \neq 1$ and $\xi_0 = 1$.

Case $\xi_0 \neq 1$. We denote as $\mathbf{u} \neq 0$ an eigenvector associate to the eigenvalue

$1/r$. Let us consider

$$\mathbf{z}(\xi) = \frac{(1-\xi)^\alpha}{\xi-\xi_0}\mathbf{u} = \left(\frac{(1-\xi)^\alpha - (1-\xi_0)^\alpha}{\xi-\xi_0} + (1-\xi_0)^\alpha \frac{1}{\xi-\xi_0}\right)\mathbf{u},$$

$$\begin{aligned}\mathbf{b}(\xi) &= \left(I - r\frac{A(\xi)}{\Gamma(\alpha)}\right)\mathbf{z}(\xi)\\ &= \frac{1}{\xi-\xi_0}\left((1-\xi)^\alpha\left(I - r\frac{A(\xi)}{\Gamma(\alpha)}\right) - (1-\xi_0)^\alpha\left(I - r\frac{A(\xi_0)}{\Gamma(\alpha)}\right)\right)\mathbf{u}.\end{aligned}$$

From Lemma 3.4, the coefficient sequence of $\mathbf{b}(\xi)$ is in c_0, while $\mathbf{z}(\xi)$ has a
170 divergent coefficient sequence. This contradicts the assumption that $r \in R$.

Case $\xi_0 = 1$. By Lemma 3.8 we have $r = 0$ or $\det(I_{m-1} - rD(1)) = 0$. If $r = 0$, then by setting $\mathbf{b}(\xi) = \mathbf{e}$, it results $\mathbf{z}(\xi) = \mathbf{e}$, whose coefficient sequence is not in c_0, which contradicts the assumption that $r \in R$. If $\det(I_{m-1} - rD(1)) = 0$, then there exists $\mathbf{u}_{m-1}$ such that $(I_{m-1} - rD(1))\,\mathbf{u}_{m-1} = \mathbf{0}$. We set

$$\mathbf{u}(\xi) = \left(\mathbf{u}_{m-1}^T, (1-\xi)^\alpha u_m\right),$$

with

$$u_m = -\mathbf{d}_2^T(1)\mathbf{u}_{m-1}.$$

Now we prove that $\mathbf{u}(\xi)$ is an eigenvector of $B\dfrac{A(\xi)}{\Gamma(\alpha)}B^{-1}$ with $\xi = 1$ corresponding to the eigenvalue $1/r$. As a matter of fact, by (3.29)

$$\left(I - rB\frac{A(\xi)}{\Gamma(\alpha)}B^{-1}\right)\mathbf{u}(\xi) = \begin{pmatrix} (I_{m-1} - rD(\xi))\,\mathbf{u}_{m-1} - r\mathbf{d}_1(\xi)(1-\xi)^\alpha u_m \\ (1-\xi)^\alpha u_m - r\mathbf{d}_2^T(\xi)\mathbf{u}_{m-1} - rd_3(\xi)(1-\xi)^\alpha u_m \end{pmatrix}. \tag{3.32}$$

From (3.30) $\lim\limits_{\xi\to 1} d_3(\xi)(1-\xi)^\alpha = 1$, then

$$\lim_{\xi\to 1}\left(I - rB\frac{A(\xi)}{\Gamma(\alpha)}B^{-1}\right)\mathbf{u}(\xi) = \begin{pmatrix} (I_{m-1} - rD(1))\,\mathbf{u}_{m-1} \\ -r\mathbf{d}_2^T(1)\mathbf{u}_{m-1} - ru_m \end{pmatrix} = \begin{pmatrix} 0 \\ 0 \end{pmatrix}.$$

Let us consider $\mathbf{z}(\xi) = (1-\xi)^{-1}B^{-1}\mathbf{u}(\xi)$, which has at least one component whose coefficient sequence is not in c_0. Then

$$\begin{aligned}\mathbf{u}(\xi) &= \left(I - r\frac{A(\xi)}{\Gamma(\alpha)}\right)\mathbf{z}(\xi) =\\ &\frac{1}{1-\xi}\left[B^{-1}\left(I - rB\frac{A(\xi)}{\Gamma(\alpha)}B^{-1}\right)\mathbf{u}(\xi) - B^{-1}\left(I - rB\frac{A(\xi)}{\Gamma(\alpha)}B^{-1}\right)\mathbf{u}(1)\right],\end{aligned}$$

which is in c_0 by Lemma (3.4) and since $\left(I - rB\frac{A(\xi)}{\Gamma(\alpha)}B^{-1}\right)\mathbf{u}(\xi)$ has coefficient sequence in ℓ^1 (compare (3.32) and (3.30)). This contradicts the assumption that $r \in R$. □

4. Stability regions

In this section, we draw stability regions of some TSSC methods, for different choices of collocation parameters and of fractional index α in the test equation (3.11). To plot the stability regions boundaries, we considered the property (compare [37]):

$$\partial\mathcal{R} \subseteq \left\{\frac{1}{z} \in \mathbb{C} | z \text{ is an eigenvalue of } \frac{A(\xi)}{\Gamma(\alpha)}, \text{ for a } \xi \text{ with } |\xi| = 1\right\}. \tag{4.1}$$

However, some curves belonging to the set in the righthand side of (4.1), may do not do not belong to the boundary of the stability domain. To exclude such curves, we plot

$$\left\{\frac{1}{z} \in \mathbb{C} | z \text{ is an eigenvalue of } \frac{A(\xi)}{\Gamma(\alpha)}, \text{ for a } \xi \text{ with } |\xi| = 1 - \varepsilon\right\}, \tag{4.2}$$

with small ε.

Moreover, we truncate to the first $N = 1000$ terms both the infinite series $\sum_{j=0}^{\infty} A_j \xi^j$ for $\xi \neq 1$, and the series $\sum_{j=0}^{\infty} BA_jB^{-1}\xi^j$ for $\xi = 1$, with B defined in (3.28). The unit circle is discretized by putting $\xi = e^{i\omega}$, with $\omega = \frac{2\pi}{500}j$, $j = 0, 1, ..., 499$.

4.1. Stability regions for $0 < \alpha < 1$

Fig. 4.1 shows stability regions of TSSC methods with $m = 1$, for $\eta = 0$ and $\eta = 0.5$, with variable α. When $\eta = 0$, the stability regions are all bounded for $\alpha = 0.1, 0.2, \ldots, 0.9$. For $\eta = 0.5$, the TSSC is $A(\alpha\frac{\pi}{2})$-stable for $\alpha = 0.1, \ldots, 0.6$, while has a bounded stability region for larger values of α. However, by choosing $\eta = 0.9$, we can get $A(\alpha\frac{\pi}{2})$-stability also for $\alpha = 0.7, 0.8$.

In Fig. 4.2 we consider $m = 1$, $\alpha = 0.25$ and $\eta = 0, 0.1, \ldots, 1$. We observe that the regions of stability increase monotonically with respect to c. In partic-

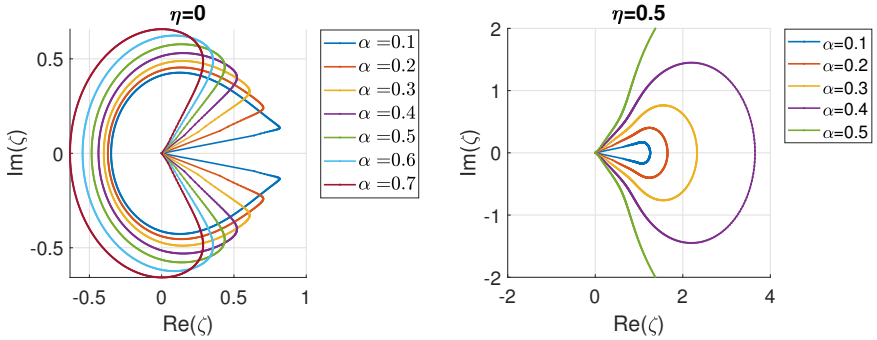

Figure 4.1: Stability regions of TSSC methods with $m = 1$. $\zeta = \lambda h^{\alpha}$. In the left figures, $\eta = 0$ and $\alpha = 0.1, 0.2, \ldots, 0.7$; the curves are the external boundaries of the stability regions. In the right figure, $\eta = 0.5$ and $\alpha = 0.1, 0.2, \ldots, 0.5$; the stability regions lie outside the plotted curves.

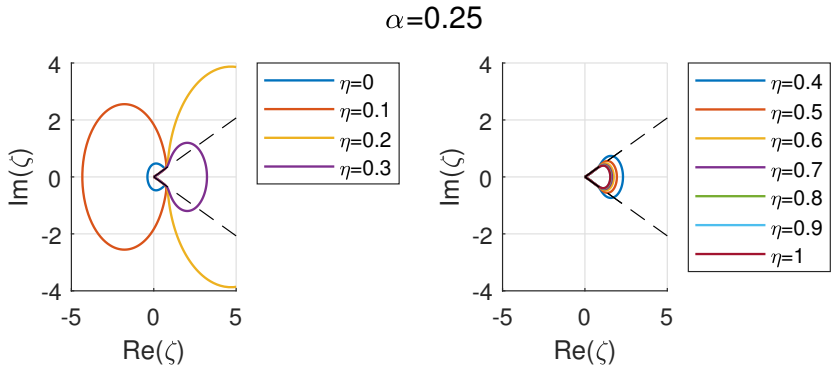

Figure 4.2: Stability regions of TSSC methods, with $m = 1$, $\alpha = 0.25$. $\zeta = \lambda h^{\alpha}$.

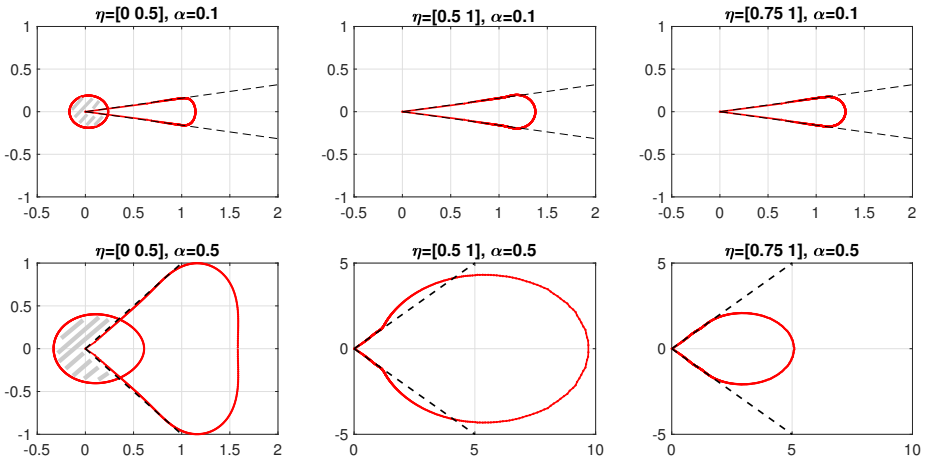

Figure 4.3: Stability regions of TSSC methods, with $m = 2$. In the left figures, the stability regions are the shaded areas; in the remaining figures, the stability regions lie outside the boundaries.

ular, TSSC methods are $A(\theta)$-stable for $\eta = 0.3, \ldots, 0.6$ and $A(\alpha\frac{\pi}{2})$-stable for $\eta = 0.7, \ldots, 1$.

By comparing stability regions of Fig. 4.1 and Fig. 4.2 with those reported in [33], for the same values of α and c, we notice that stability regions of TSSC methods are smaller than those of one-step methods of same type. However, in the cases under investigation, for a fixed value of α, it is possible to obtain $A(\alpha\frac{\pi}{2})$-stable TSSC methods by a suitable choice of c.

In Fig. 4.3 we plot TSSC methods with $m = 2$, for $\alpha = 0.1$ and $\alpha = 0.5$, $\eta = [0, 0.5], [0.5, 1], [0.75, 1]$. In the case $\eta = [0, 0.5]$, to recognize which curves compose the stability region boundary, we plotted curves (4.2) and we shaded the resulting stability regions. When $\alpha = 0.1$, the TSSC is $A(\alpha\frac{\pi}{2})$-stable for $\eta = [0.5, 1], [0.75, 1]$. When $\alpha = 0.5$, the TSSC is $A(\alpha\frac{\pi}{2})$-stable for $\eta = [0.75, 1]$; is $A(\theta)$-stable for $\eta = [0.5, 1]$.

For the same values of α and of the abscissae c, stability regions of TSSC methods are usually smaller than those of one step collocation methods. This is not surprising, since it is a typical behaviour of multistep methods, when applied to ODEs, to have worse stability properties. However, in general, when

OSSC methods are $A(\alpha\frac{\pi}{2})$-stable or have an unbounded stability region, the same holds for TSSC methods, for a suitable choice of collocation parameters. Therefore, the considerable gain in accuracy justifies the advantage of TSSC methods.

By a comparison with a wider range of methods, as for example product integration, fractional BDF, fractional trapezoidal, Newton-Gregory methods studied in [7], which are $A(\alpha\frac{\pi}{2})$-stable, we observe that our methods have the same strong stability property, once the collocation parameters are properly set.

4.2. Stability regions for $1 < \alpha < 2$

Fig. 4.4 and Fig. 4.5 show stability regions of TSSC method with $m = 1$ and collocation parameter $\eta = 0$ and $\eta = 0.5$, respectively, with variable α. In all cases, the stability regions are bounded. For $\eta = 0$, when $\alpha < 1.5$, the interval of stability (i.e. the intersection of the stability region with the real axis) is increasing with α; for $\alpha \geq 1.5$, the stability regions decrease with α. For $\eta = 0.5$ the stability regions are larger with respect to the case $\eta = 0$; moreover their areas decrease with α.

In Fig. 4.6 we fixed $\alpha = 1.25$ and let η vary in $[0, 1]$. All regions are bounded and increase with η.

In Fig. 4.7 we plotted stability regions for TSSC methods with $m = 2$, $\alpha = 1.1$ and 1.5, $\eta = [0, 0.5], [0.5, 1]$ and $[0.5, 1]$. Stability regions are larger when collocation parameters are closer to 1, while no significant differences are noticed with respect to α.

To draw some conclusion for the case $1 < \alpha < 2$, we observe that the stability regions we constructed are considerably large in most cases, although bounded. Therefore, if a non-stiff or a mild stiff problem with $\alpha \in (1, 2)$ is considered, TSSC methods do not require strict limitations for the stepsize (e.g. see numerical results shown in Figures 5.5 and 5.6). Moreover, a similar change in the stability properties from the case $\alpha \in (0, 1)$ to the case $\alpha \in (1, 2)$ has been registered also for other classes of methods, e.g. product integration methods and Newton-Gregory formulas lose $A(\alpha\pi/2)$-stability when $\alpha > 1$ (compare [7]).

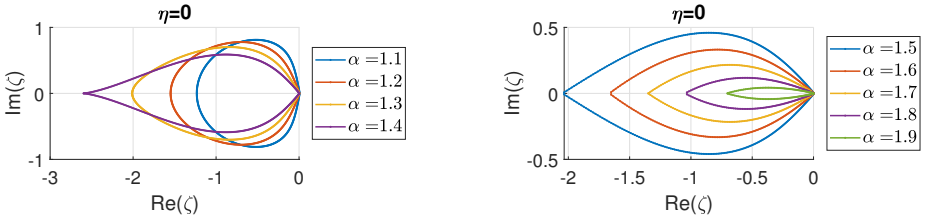

Figure 4.4: Stability regions of TSSC methods with $m = 1$ and $\eta = 0$. $\zeta = \lambda h^\alpha$. The stability regions lie inside the plotted curves.

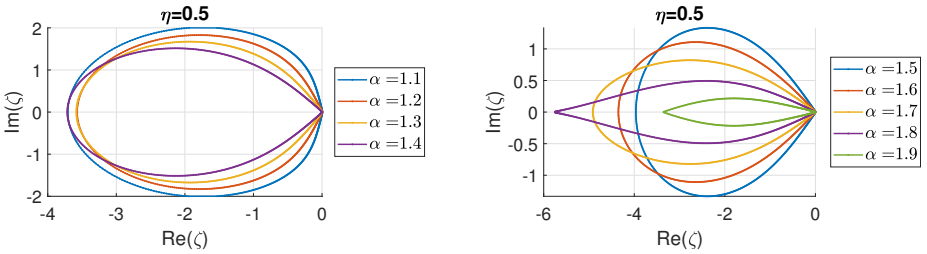

Figure 4.5: Stability regions of TSSC methods with $m = 1$ and $\eta = 0.5$. $\zeta = \lambda h^\alpha$. The stability regions lie inside the plotted curves.

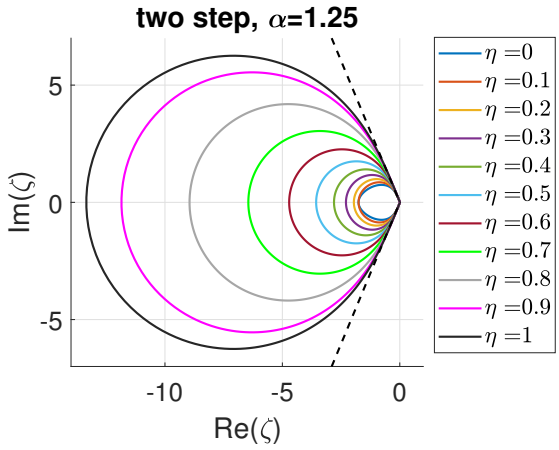

Figure 4.6: Stability regions of TSSC methods with $m = 1$ and $\alpha = 1.25$ and c varying in $[0, 1]$. $\zeta = \lambda h^\alpha$. The stability regions lie inside the closed curves. The dashed lines are the boundaries of the Σ_α stability region (3.12).

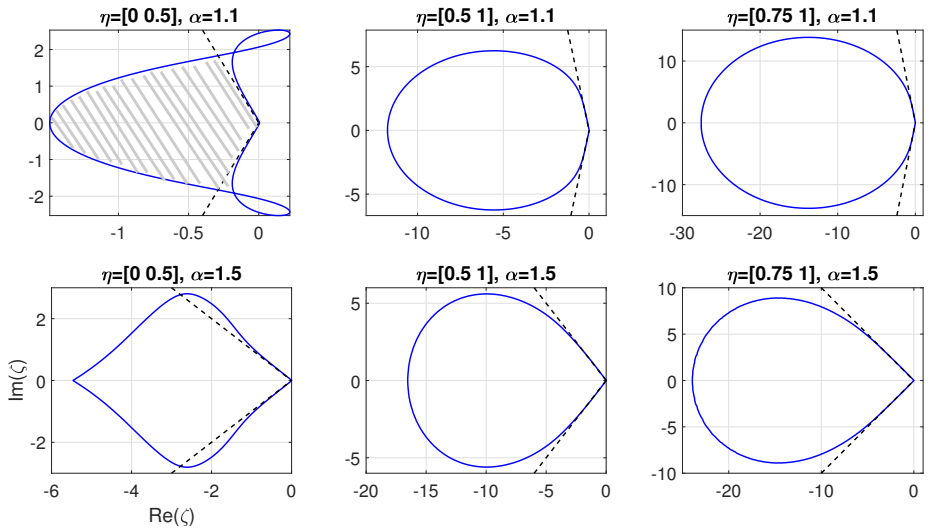

Figure 4.7: Stability regions of TSSC methods with $m = 2$. $\zeta = \lambda h^{\alpha}$. In the left top figure, the stability region is the shaded area, in the remaining figures, the stability regions lie inside the closed curves. The dashed lines are the boundaries of the Σ_{α} stability region (3.12).

5. Numerical experiments

Here we apply TSSC methods on a selection of test problems, to confirm theoretical expectations in a constant stepsize implementation and to show usefulness of stability results when a graded mesh is adopted. In the following experiments, we compute the absolute error

$$error(t) = |y(t) - y_N(t)|, \qquad t \in [0, b],$$

and the relative error

$$E_{\infty}^{rel} = \frac{\max_{n=0,\dots,N} |y(t_n) - y_N(t_n)|}{\max_{n=0,\dots,N} |y(t_n)|},$$

where $y(t)$ is the analytical solution or a reference numerical solution, while $y_N(t)$ is defined in (3.8).

We performed all the numerical experiments in MATLAB, by using the codes illustrated in [32, 34].

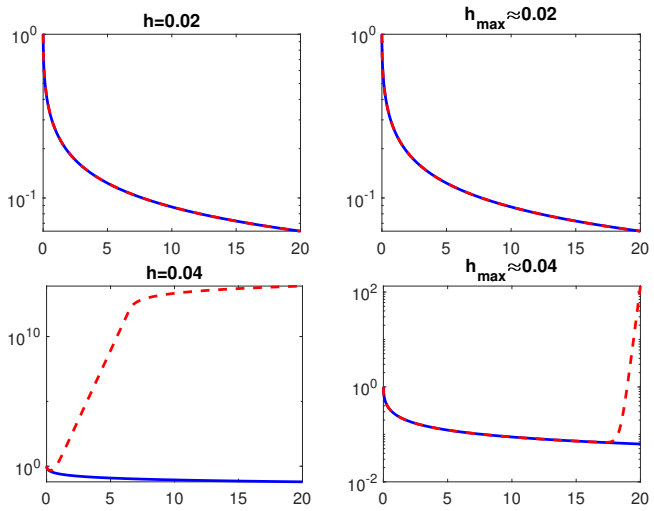

Figure 5.1: Example 5.1 with $\alpha = 0.5$ and $\lambda = -2$. Exact solution (solid line) and numerical one (dashed line) obtained by TSSC with $\eta = [0, 0.5]$. In the left figures the stepsize is constant, while in the right figures a graded mesh is used, with $r = 8$. Logarithmic scale on the y-axis.

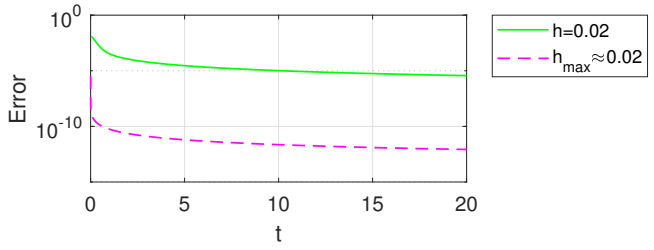

Figure 5.2: Example 5.1 with $\alpha = 0.5$ and $\lambda = -2$. Errors of the numerical solution of TSSC with $\eta = [0, 0.5]$, with constant stepsize $h = 0.02$ (solid line), and with graded mesh with $r = 8$ and $h_{max} \approx 0.02$ (dashed line). Logarithmic scale on the y-axis.

Example 5.1. *Basic test equation*

The first problem is (3.11), with $y_0 = 1$; $\alpha = 0.5$ or $\alpha = 1.5$; $b = 20$ or $b = 80$. Th. 2.1 holds for with $\nu = 0.5$ and arbitrary $q \in \mathbb{N}$ (for both values of α and b). Thus, the TSSC has an error decay $O(N^{-2m})$ if the grading exponent $r \geq 4m$.

Figures 5.1 and 5.2 show the results obtained on Example 5.1 with $\alpha = 0.5$, $\lambda = -2$, by the TSSC with $m = 2$ and $\eta = [0, 0.5]$. For the constant stepsize $h = 0.02$, $\lambda h^\alpha \approx -0.2828$, which is inside the stability region; while for $h = 0.04$, $\lambda h^\alpha = -0.4$, which is outside the stability region. In agreement with the theoretical expectations, in the former case the method is stable, while in the latter case, some instability arises. A similar behavior is observed for the graded mesh case, where the error is considerably smaller, as it can be seen by Figure 5.2.

In Figure 5.3 we applied the TSSC with $m = 2$ and $\eta = [0.75, 1]$ to Example 5.1 with $\alpha = 0.5$, $\lambda = -1000$. This method is $A(\alpha\frac{\pi}{2})$-stable, thus the error is bounded also for a large value of the stepsize. We also plot the errors in Fig. 5.4.

Secondly, we consider Example 5.1 with $\alpha = 1.5$ and $\lambda = -100$, solved by the TSSC with $m = 2$ and $\eta = [0, 0.5]$ In Figures 5.5 and 5.6 we plotted the analytical and numerical solutions, and the absolute error, respectively. For the constant stepsize, when $h = 0.1$, $\lambda h^\alpha \approx -3.16$, which is inside the stability region; while for $h = 0.2$, $\lambda h^\alpha = -8.9$, which is outside the stability region. As expected, the numerical solution shows instability when $h = 0.2$, both in the case of graded or constant stepsize.

Example 5.2. *Nonlinear fractional differential equation* [taken from 24]

$$D^\alpha y(t) = \lambda y + \rho y(1 - y^2) + g(t), \quad t \in (0, b], \qquad y(0) = y_0, \qquad (5.1)$$

with $\alpha = 0.15$, $\lambda = -3$, $\rho = 0.8$, $b = 8$ and $y_0 = 2$. $g(t)$ is such that the solution of (5.1) is $y(t) = y_0 + \sum_{k=1}^{6} t^{\sigma_k}$, with $\sigma_k = k\alpha$, $k = 1, \ldots, 5$, and $\sigma_6 = 2 + \alpha$.

Assumptions of Th. 2.1 are satisfied with $\nu = 1 - \alpha = 0.85$ and any $q \in \mathbb{N}$.

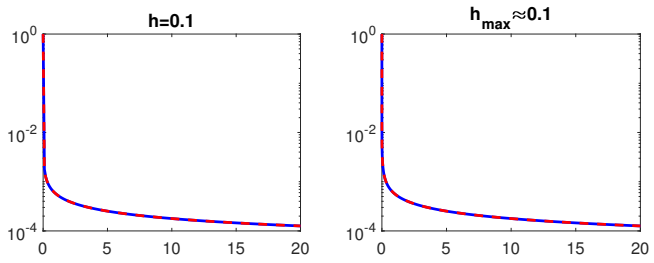

Figure 5.3: Example 5.1 with $\alpha = 0.5$ and $\lambda = -1000$. Exact solution (solid line) and numerical one (dashed line) obtained by TSSC with $\eta = [0.75, 1]$. On the left the stepsize is constant, on the right the mesh is graded and $r = 8$. Logarithmic scale on the y-axis.

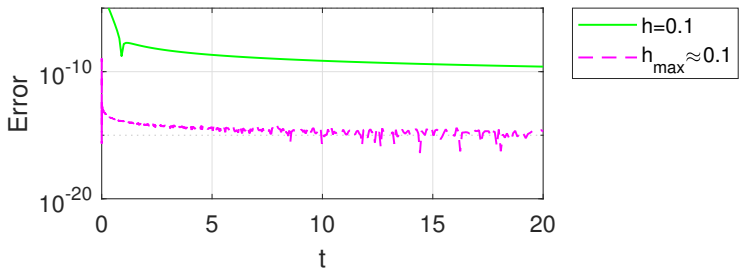

Figure 5.4: Example 5.1 with $\alpha = 0.5$ and $\lambda = -1000$. Errors of the numerical solution of TSSC with $\eta = [0.75, 1]$, with constant stepsize $h = 0.1$ (solid line), and with graded mesh with $r = 8$ and $h_{max} \approx 0.1$. Logarithmic scale on the y-axis.

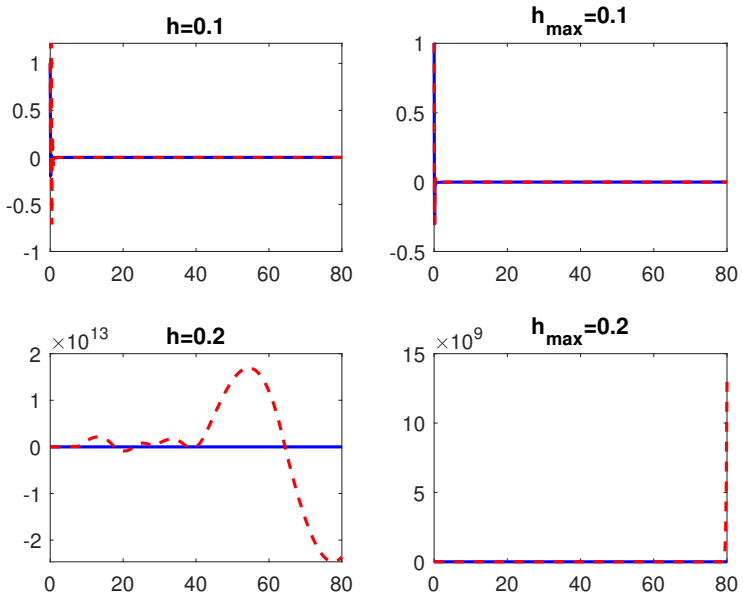

Figure 5.5: Example 5.1 with $\alpha = 1.5$ and $\lambda = -100$. Errors of the numerical solution of TSSC with $\eta = [0, 0.5]$. Exact solution (solid line) and numerical one (dashed line) obtained by TSSC with $\eta = [0, 0.5]$. In the left figures the stepsize is constant, while in the right figures a graded mesh is used, with $r = 8$. Logarithmic scale on the y-axis.

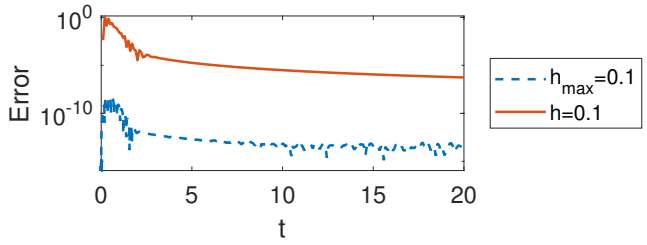

Figure 5.6: Example 5.1 with $\alpha = 1.5$ and $\lambda = -100$. Errors of the numerical solution of TSSC with $\eta = [0, 0.5]$, with constant stepsize $h = 0.1$ (solid line), and with graded mesh with $r = 8$ and $h_{max} \approx 0.1$ (dashed line). Logarithmic scale on the y-axis.

Therefore, the error of the TSSC decreases with rate $O(N^{-2m})$, whenever $r \geq \frac{40}{3}m = 13.\bar{3}m$.

We consider the following methods:

- OSSC1, i.e. the OSSC method [17] with $m = 2$, $\eta = \left[\frac{3\pm\sqrt{3}}{6}\right]$ and $r = 7.17$;
- TSSC1, i.e. the TSSC method (3.4)(3.6)(3.8) with $m = 2$, $\eta = [0.75, 1]$ and $r = 26.7$.
- TSSC2, i.e. the TSSC method (3.4)(3.6)(3.8) with $m = 2$, $\eta = [0, 0.5]$ and $r = 26.7$.

The one-step method OSSC1 is superconvergent, as a matter of fact the error decays as $O(N^{-(m+\alpha)}) = O(N^{-2.15})$ [17]; while the error of methods TSSC1 and TSSC2 decays with rate $O(N^{-2m}) = O(N^{-4})$. TSSC2 has a bounded stability region for $\alpha = 0.15$. Both OSSC1 and TSSC1 are $A(\alpha\frac{\pi}{2})$-stable for $\alpha = 0.15$, thus they are stable also for large stepsizes, as it is confirmed by Table 1. Moreover we observe that the error of method TSSC1 is much smaller, since the decay rate is higher.

We observe that, as for the ODEs, good linear stability properties are essential to obtain acceptable results in the nonlinear cases. As a matter of fact, if we solve the test example 5.2 by method TSSC2, which has a bounded stability region, the numerical solution blows up, as seen in Fig. 5.7. On the other hand, when we apply the method TSSC1, which is $A(\alpha\frac{\pi}{2})$-stable, the numerical solution is highly accurate (see Fig. 5.7 and Table 1).

6. Conclusions

In this paper we carried out the study of numerical stability of TSSC methods, introduced by [9]. The stability domain has been characterized by the eigenvalues of a formal power series, whose coefficients depend on the method parameters. Several stability regions have been constructed and $A(\alpha\frac{\pi}{2})$-stable methods have been found. Theoretical limitations on the stepsize proved to be

Table 1: Relative error E_{∞}^{rel} on Example 5.2.

	OSSC1		TSSC1	
N	$h_{\max}$	E_{∞}^{rel}	$h_{\max}$	E_{∞}^{rel}
$b/2^{-4}$	0.4375	2.71E-04	0.7981	1.7547e-10
$b/2^{-5}$	0.2214	6.28E-05	0.4088	1.4545e-11
$b/2^{-6}$	0.1114	1.43E-05	0.2069	1.1637e-12
$b/2^{-7}$	0.0558	3.25E-06	0.1041	8.9151e-14

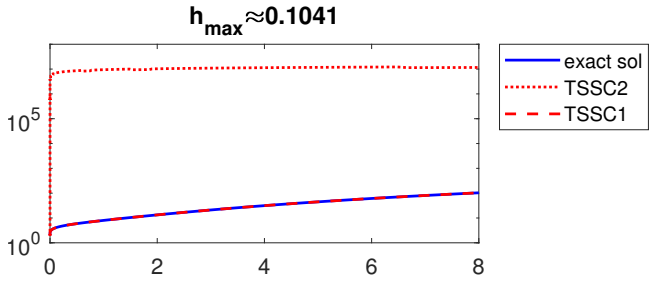

Figure 5.7: Exact and numerical solutions for Example 5.2.

quite sharp not only for constant stepsize applications, but also for graded mesh implementations.

Acknowledgements

The authors are members of the INdAM Research group GNCS. This work is supported by GNCS-INDAM project and by PRIN2017-MIUR project.

References

[1] A. A. Kilbas, H. M. Srivastava, J. J. Trujillo, Theory and applications of fractional differential equations, volume 204 of *North-Holland Mathematics Studies*, Elsevier Science B.V., Amsterdam, 2006.

[2] F. Mainardi, Fractional calculus and waves in linear viscoelasticity, Imperial College Press, London, 2010. URL: `http://dx.doi.org/10.1142/`

9781848163300. doi:10.1142/9781848163300, An introduction to mathematical models.

[3] I. Podlubny, Fractional differential equations, volume 198 of *Mathematics in Science and Engineering*, Academic Press, Inc., San Diego, CA, 1999. An introduction to fractional derivatives, fractional differential equations, to methods of their solution and some of their applications.

[4] K. Diethelm, N. J. Ford, A. D. Freed, A predictor-corrector approach for the numerical solution of fractional differential equations, Nonlinear Dynam. 29 (2002) 3–22. Fractional order calculus and its applications.

[5] K. Diethelm, N. J. Ford, A. D. Freed, Detailed error analysis for a fractional Adams method, Numer. Algorithms 36 (2004) 31–52.

[6] R. Garrappa, On linear stability of predictor-corrector algorithms for fractional differential equations, Int. J. Comput. Math. 87 (2010) 2281–2290.

[7] R. Garrappa, Trapezoidal methods for fractional differential equations: theoretical and computational aspects, Math. Comput. Simulation 110 (2015) 96–112.

[8] K. Burrage, A. Cardone, R. D'Ambrosio, B. Paternoster, Numerical solution of time fractional diffusion systems, Appl. Numer. Math. 116 (2017) 82–94.

[9] A. Cardone, D. Conte, B. Paternoster, Two-step collocation methods for fractional differential equations, Discrete Contin. Dyn. Syst. Ser. B 23 (2018) 2709–2725.

[10] X. Li, Numerical solution of fractional differential equations using cubic B-spline wavelet collocation method, Commun. Nonlinear Sci. Numer. Simul. 17 (2012) 3934–3946.

[11] M. Lakestani, M. Dehghan, S. Irandoust-pakchin, The construction of operational matrix of fractional derivatives using B-spline functions, Commun. Nonlinear Sci. Numer. Simul. 17 (2012) 1149–1162.

[12] J. Liu, H. Fu, X. Chai, Y. Sun, H. Guo, Stability and convergence analysis of the quadratic spline collocation method for time-dependent fractional diffusion equations, Appl. Math. Comput. 346 (2019) 633–648.

[13] L. Pezza, F. Pitolli, A fractional spline collocation-Galerkin method for the time-fractional diffusion equation, Commun. Appl. Ind. Math. 9 (2018) 104–120.

[14] E. Pellegrino, L. Pezza, F. Pitolli, A collocation method in spline spaces for the solution of linear fractional dynamical systems, Math. Comput. Simulation 176 (2020) 266–278.

[15] A. Pedas, E. Tamme, On the convergence of spline collocation methods for solving fractional differential equations, J. Comput. Appl. Math. 235 (2011) 3502–3514.

[16] A. Pedas, E. Tamme, Spline collocation methods for linear multi-term fractional differential equations, J. Comput. Appl. Math. 236 (2011) 167–176.

[17] A. Pedas, E. Tamme, Numerical solution of nonlinear fractional differential equations by spline collocation methods, J. Comput. Appl. Math. 255 (2014) 216–230.

[18] A. Pedas, E. Tamme, Spline collocation for nonlinear fractional boundary value problems, Appl. Math. Comput. 244 (2014) 502–513.

[19] M. Zayernouri, G. E. Karniadakis, Fractional spectral collocation method, SIAM J. Sci. Comput. 36 (2014) A40–A62.

[20] V. Daftardar-Gejji, H. Jafari, Adomian decomposition: a tool for solving a system of fractional differential equations, J. Math. Anal. Appl. 301 (2005) 508–518.

[21] G.-c. Wu, E. W. M. Lee, Fractional variational iteration method and its application, Phys. Lett. A 374 (2010) 2506–2509.

[22] G.-c. Wu, A fractional variational iteration method for solving fractional nonlinear differential equations, Comput. Math. Appl. 61 (2011) 2186–2190.

[23] Y. Nawaz, Variational iteration method and homotopy perturbation method for fourth-order fractional integro-differential equations, Comput. Math. Appl. 61 (2011) 2330–2341.

[24] W. Cao, F. Zeng, Z. Zhang, G. E. Karniadakis, Implicit-explicit difference schemes for nonlinear fractional differential equations with nonsmooth solutions, SIAM J. Sci. Comput. 38 (2016) A3070–A3093.

[25] H. Brunner, P. J. van der Houwen, The numerical solution of Volterra equations, volume 3 of *CWI Monographs*, North-Holland Publishing Co., Amsterdam, 1986.

[26] H. Brunner, A. Pedas, G. Vainikko, Piecewise polynomial collocation methods for linear Volterra integro-differential equations with weakly singular kernels, SIAM J. Numer. Anal. 39 (2001) 957–982 (electronic).

[27] H. Brunner, Collocation methods for Volterra integral and related functional differential equations, volume 15 of *Cambridge Monographs on Applied and Computational Mathematics*, Cambridge University Press, Cambridge, 2004. URL: `http://dx.doi.org/10.1017/CBO9780511543234`. doi:`10.1017/CBO9780511543234`.

[28] U. Ascher, Collocation for two-point boundary value problems revisited, SIAM J. Numer. Anal. 23 (1986) 596–609.

[29] C. de Boor, B. Swartz, Collocation at Gaussian points, SIAM J. Numer. Anal. 10 (1973) 582–606.

[30] R. D. Russell, L. F. Shampine, A collocation method for boundary value problems, Numer. Math. 19 (1972) 1–28.

[31] L. Blank, Numerical treatment of differential equations of fractional order, Technical Report, University of Manchester, Department of Mathematics, 1996. Numerical Analysis Report.

[32] A. Cardone, D. Conte, B. Paternoster, A MATLAB implementation of spline collocation methods for fractional differential equations, Lect. Notes Comput. Sci. 12949 LNCS (2021) 387–401.

[33] A. Cardone, D. Conte, Stability analysis of spline collocation methods for fractional differential equations, Math. Comput. Simulat. 178 (2020) 501 – 514.

[34] A. Cardone, D. Conte, B. Paternoster, A MATLAB code for fractional differential equations based on two-step spline collocation methods, Springer INdAM Series (2022). To appear.

[35] E. A. Rawashdeh, Numerical solution of fractional integro-differential equations by collocation method, Appl. Math. Comput. 176 (2006) 1–6.

[36] L. Blank, Stabilitätsanalyse der Kollokationsmethode für Volterra-Integral-Gleichungen mit schwach singulärem Kern, 227, Rheinische Friedrich-Wilhelms-Universität Bonn, 1991.

[37] L. Blank, Stability of collocation for weakly singular Volterra equations, IMA J. Numer. Anal. 15 (1995) 357–375.

[38] C. Lubich, A stability analysis of convolution quadratures for Abel-Volterra integral equations, IMA J. Numer. Anal. 6 (1986) 87–101.

[39] K. Diethelm, The analysis of fractional differential equations, volume 2004 of *Lecture Notes in Mathematics*, Springer-Verlag, Berlin, 2010. URL: `http://dx.doi.org/10.1007/978-3-642-14574-2`. doi:`10.1007/978-3-642-14574-2`, an application-oriented exposition using differential operators of Caputo type.

[40] L. Galeone, R. Garrappa, Explicit methods for fractional differential equations and their stability properties, J. Comput. Appl. Math. 228 (2009) 548–560.

[41] W. Cao, Z. Zhang, G. E. Karniadakis, Time-splitting schemes for fractional differential equations I: smooth solutions, SIAM J. Sci. Comput. 37 (2015) A1752–A1776.

[42] A. Zygmund, Trigonometric series. 2nd ed. Vols. I, II, Cambridge University Press, New York, 1959.

[43] A. Erdélyi, W. Magnus, F. Oberhettinger, F. G. Tricomi, Higher transcendental functions. Vol. I, Robert E. Krieger Publishing Co., Inc., Melbourne, Fla., 1981. Based on notes left by Harry Bateman, With a preface by Mina Rees, With a foreword by E. C. Watson, Reprint of the 1953 original.